Paleoceanography and Paleoclimatology

RESEARCH ARTICLE
10.1029/2019PA003712

Key Points:
- Phytoplankton biomass has increased in north-western Australia by 1.5–3 times since the 1950s
- Fifty-six percent of the phytoplankton variance was related to increases in SST and rainfall and 20.4% to the Interdecadal Pacific Oscillation
- We empirically predict a more productive coastal environment in north-western Australia in coming decades

Supporting Information:
- Supporting Information S1

Correspondence to:
D. Liu, and J. K. Keesing,dyliu@sklec.ecnu.edu.cnjohn.keesing@csiro.au

Citation:
Yuan, Z., Liu, D., Masqué, P., Zhao, M., Song, X., & Keesing, J. K. (2020). Phytoplankton responses to climate-induced warming and interdecadal oscillation in North-Western Australia. *Paleoceanography and Paleoclimatology*, *35*, e2019PA003712. https://doi.org/10.1029/2019PA003712

Received 4 JUL 2019
Accepted 5 FEB 2020
Accepted article online 8 FEB 2020

Phytoplankton Responses to Climate-Induced Warming and Interdecadal Oscillation in North-Western Australia

Zineng Yuan[1], Dongyan Liu[2], Pere Masqué[3,4,5], Meixun Zhao[6], Xiuxian Song[7], and John K. Keesing[8]

[1]CAS Key Laboratory of Coastal Environmental Processes and Ecological Remediation, Yantai Institute of Coastal Zone Research, Chinese Academy of Sciences/Shandong Provincial Key Laboratory of Coastal Zone Environmental Processes, Yantai, China, [2]State Key Laboratory of Estuarine and Coastal Research, East China Normal University, Shanghai, China, [3]School of Science and Centre for Marine Ecosystems Research, Edith Cowan University, Joondalup, Western Australia, Australia, [4]Institut de Ciència i Tecnologia Ambientals and Departament de Física, Universitat Autònoma de Barcelona, Barcelona, Spain, [5]Oceans Institute and School of Physics, The University of Western Australia, Crawley, Western Australia, Australia, [6]Laboratory of Marine Chemistry Theory and Technology, Ministry of Education/Institute for Advanced Ocean Study, Ocean University of China, Qingdao, China, [7]Key Laboratory of Marine Ecology and Environmental Sciences, Institute of Oceanology, Chinese Academy of Sciences/Laboratory of Marine Ecology and Environmental Science, Qingdao National Laboratory for Marine Science and Technology, Qingdao, China, [8]CSIRO Oceans and Atmosphere Research and Oceans Institute, Indian Ocean Marine Research Centre, The University of Western Australia and Western Australian Marine Science Institution, Crawley, Western Australia, Australia

Abstract Growing evidence has suggested that ocean warming could cause a decline in marine phytoplankton productivity. However, studies in tropical waters have discovered that evolutionary adaptation of local species to warming and positive response to increasing rainfall could avoid the sharp decline in productivity. Here, the decadal trends of phytoplankton biomass, reconstructed using the biomarkers of brassicasterol (diatoms) and dinosterol (dinoflagellates), showed a 1.5–3 times increase since the 1950s along a large section of the Kimberley coast, north-western Australia. Principal component analysis found that 56% of the phytoplankton variance was linked with climate change-induced increases in sea surface temperature and rainfall associated with increased tropical cyclones, which can enhance nutrient supply favoring phytoplankton growth and production; 20.4% of the phytoplankton variance tended to be related to the Interdecadal Pacific Oscillation through a mechanism of ocean-coast interaction. We empirically predict that the negative impact of rising temperatures on phytoplankton in north-western Australia could be buffered by the increasing tropical cyclones and the coming warm phase of Interdecadal Pacific Oscillation.

1. Introduction

Phytoplankton assemblages in the ocean play an essential role in primary production, biogeochemical cycling, and food webs (Field et al., 1998). In October 2018, the Intergovernmental Panel on Climate Change (IPCC) released a report on the impacts of global warming >1.5 °C above preindustrial levels (IPCC SR 1.5). Changes in temperature force not only the shift of phytoplankton distribution but also their composition and abundance (Hays et al., 2005). For example, warmer water is thought to favor many cyanobacterial and dinoflagellate species and smaller-sized cells (Paerl & Scott, 2010), as they are efficient at harvesting light and nutrients and maintaining their position in the eutrophic zone (Finkel et al., 2010). Warmer water in the open sea is able to enhance the intensity of stratification and reduce the nutrient supply in the mixed layer, and consequently reduces phytoplankton productivity (Behrenfeld et al., 2006; Henson et al., 2010; Martinez et al., 2009). In coastal waters, the shift in phytoplankton is often linked to the overlapping effects of warming and nutrient enrichment (Boyce & Worm, 2015). Warmer temperature can alter the chemical composition of the cell, adjust the phytoplankton demand for N and P, and increase the opportunity for harmful algal bloom species (Yvon-Durocher et al., 2015).

The Kimberley coast, located in north-western Australia, has been identified as one of the world's least human-impacted coastal areas (Halpern et al., 2008). It is also one of the most ecologically valuable

marine regions in Australia, supporting a large range of marine habitat types including mangrove, seagrass beds, and coral reefs, which in turn harbor richly diverse invertebrate, fish, reptile, and marine mammal faunas (Keesing, 2014; Keesing et al., 2011; Wilson, 2013; Woinarski et al., 2007). However, north-western Australia is experiencing significant climate change, for example, annual average sea surface temperature (SST) increased approximately 0.6 °C over the past 50 years (Lough, 2008); annual rainfall showed a noticeable increase over recent decades (*Taschetto and England*, 2007; O'Donnell et al., 2015); the frequency, average maximum intensity, and duration of severe tropical cyclones have increased since 1990 (Hassim & Walsh, 2008; Lavender & Abbs, 2013). Moreover, the El Niño Southern Oscillation (ENSO) shows a profound impact on the Kimberley marine ecosystem (Furnas, 2007; Thompson et al., 2015). For example, the Indonesian Throughflow (ITF) transport along the shelf of northwest Australia has been discovered to match the ENSO cycle (Meyers, 1996). The interannual variation of phytoplankton productivity shows higher values during the El Niño years and lower values during the La Niña years (Furnas, 2007; Thompson et al., 2015). The Interdecadal Pacific Oscillation (IPO), described as interdecadal variability of ENSO, can strengthen or weaken the ENSO-driven changes in north-western Australia (Mantua et al., 1997; Power et al., 1999). The ITF transport over the past 50 years has shown interdecadal oscillations following the warm and cold patterns of the IPO (Feng et al., 2011; Wainwright et al., 2008).

Previous studies reported that fast adaptation of tropical phytoplankton to warming can avoid the sharp decline of phytoplankton diversity and production in tropical waters (Jin & Agustí, 2018; Schlüter et al., 2014). The findings support field observations in northern Australia, where there was a twofold increase in primary productivity between the 1960s and 1990s (Furnas & Carpenter, 2016). However, it is still hard to evaluate the multiple impacts of climate-induced warming, rainfall, and interdecadal oscillation on phytoplankton trend in north-western Australia, due to the lack of decadal observation data. Paleoecological methods, using the geochemical and biological proxies preserved in sediment cores, offer an effective pathway to acquire environmental and ecological information on decadal scales. Brassicasterol and dinosterol in the sediment are reliable biomarkers to reconstruct the biomasses of diatoms and dinoflagellates, respectively, due to their biosynthetic specificity and resistance to degradation (Volkman et al., 1998). Despite the recognized potential biases linked to degradation effect or depositional process, the application of these methods in coastal waters of north-western Australia has proven the feasibility of using phytoplankton biomarkers as proxies to reconstruct historical phytoplankton biomass (Burns et al., 2003; Yuan et al., 2018).

The analysis of biomarker sterols has supported significant findings in understanding long-term phytoplankton variations in response to climate change. For example, in Kyllaren Fjord, Smittenberg et al. (2004) found significant increases of primary production during the past 400 years by using sterols together with stable carbon isotopic composition; Xing et al. (2016) used the ratio of brassicasterol and dinosterol to understand the phytoplankton community changes in response to Pacific Decadal Oscillation in the East China Sea. In this study, sediment cores were collected from three bays along the Kimberley coastline, in north-western Australia, including Roebuck Bay off Broome, Koolama Bay off King George River, and Cygnet Bay in King Sound (Figure 1). The total organic carbon (TOC), the biomarkers of diatom (brassicasterol), and dinoflagellate (dinosterol) preserved in sediment cores were analyzed and used to describe the spatiotemporal patterns of diatom and dinoflagellate biomasses on decadal scales. Our study assumed that rising SST, increasing rainfall, and shifting IPO phases were the main climate drivers of decadal variations of diatom and dinoflagellate biomass. Their correlations were evaluated via statistical analysis, aimed at better understanding the different responses of phytoplankton to regional climatic drivers in the context of global warming.

2. Materials and Methods

2.1. Study Area and Core Information

The Kimberley coastline is more than 20,000 km long, covering latitudes of 15–20° and longitudes of 121–129° in north-western Australia (Wilson, 2013; Woinarski et al., 2007). It is characterized by a distinct monsoonal regime, with a wet summer season between November and April and a dry winter season between May and October. The hydrodynamic processes in coastal waters are strongly impacted by surface circulation, tidal action, and tropical cyclones. During February to June, the ITF brings warmer and lower salinity seawater southwestward to the coast of north-western Australia; while during the rest

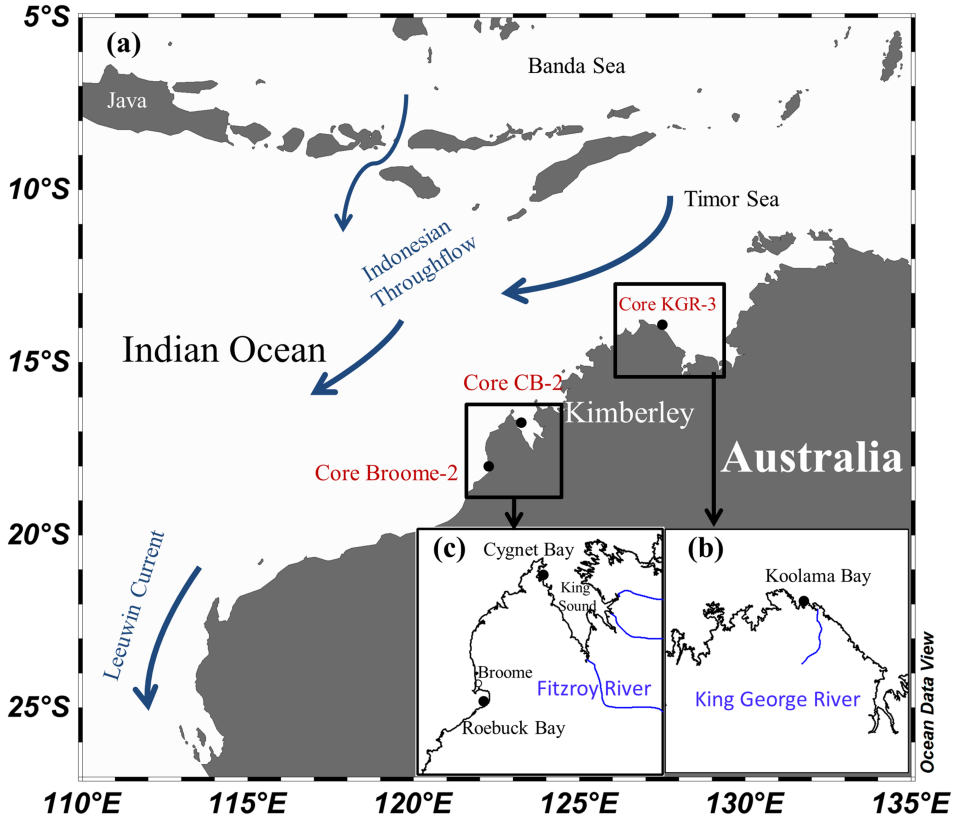

Figure 1. A: a schematic map showing three sampling sites (●: Core Broome-2, Core CB-2, and Core KGR-3) along the Kimberley coastline and the dominant current systems in North-Western Australia (Indonesia Throughflow and Leeuwin current). B: location of Core KGR-3 (Koolama Bay off King George River). C: locations of Core Broome-2 (Roebuck Bay off Broome) and Core CB-2 (Cygnet Bay in king sound).

of the year, strong winds from the southwest often cause intermittent reversals of the ITF with occasional intrusion of cold deep water into the coastal waters (Holloway & Nye, 1985). During the wet season, a high frequency of tropical cyclones results in episodes of very high rainfall, which can account for over 40% of annual precipitation (Lavender & Abbs, 2013), and more than 100 streams and rivers discharge significant freshwater (30,000 GL/year) into the coastal area (Woinarski et al., 2007). The Kimberley coast has the second largest tidal range in the world with the maximum tidal range reached 11.7 m (Holloway, 1983; Wolanski & Spagnol, 2003). Thus, the coastal waters in the Kimberley are mainly controlled by tide-driven currents; meanwhile, they are impacted by the variability of the ITF and tropical cyclones on seasonal scales.

Sediment cores at three locations were collected using a push corer by SCUBA diving in 2011 and a Vibecore-D corer on the research vessel RV Solander of the Australian Institute of Marine Science in 2013 and 2014 (Figure 1(a)). Core KGR-3 is from Koolama Bay (127°8′E, 13°53′S, water depth 13 m, core length 123 cm). Koolama Bay is located off King George River in northern Kimberley with an approximate area of 30 km^2 (Figure 1(b)). It receives freshwater from King George River and has an annual temperature range of 26.1–28.9 °C, an annual rainfall range of 700–1,800 mm, and a tidal range of 3.3 m (data from the Australian Bureau of Meteorology). Core Broome-2 is from Roebuck Bay (122°17′E, 18°4′S; water depth: 14 m, core length: 136 cm), and Core CB-2 is from Cygnet Bay (122°59′E, 16°32′S, water depth 9.8 m, core length 106 cm). Roebuck Bay off the city of Broome (area: ~550 km^2) and Cygnet Bay in the King Sound (area: ~180 km^2) are located in southern Kimberley (Figure 1(c)). These sites have an annual mean temperature range of 26.0–28.4 °C, an annual rainfall range of 600–1,000 mm, and tidal range up to 11.7 m (data from the Australian Bureau of Meteorology). The Fitzroy River discharges 7,035 GL/year freshwater into King Sound (data from the Western Australian Department of Water, station: Fitzroy River-Willare), while no large rivers flow directly into Roebuck Bay.

The cores were sectioned into subsamples at 1-cm intervals and stored in a freezer at −20 °C before dating and chemical analysis. The data of Core CB-2, including chronology, grain size, TOC, and biomarkers, were published in Liu et al. (2016) and Yuan et al. (2018). Here we only used previously published data from Core CB-2 to do comparative and statistical analysis with the new data from Core Broome-2 and Core KGR-3.

2.2. Radiometric Analyses

The concentration profiles of ^{210}Pb for Core KGR-3 and Core Broome-2 were determined through the measurement of ^{210}Po in radioactive equilibrium at Edith Cowan University, following the method described in Sánchez-Cabeza et al. (1998). Briefly, aliquots of 100–200 mg were totally digested in acid media using an analytical microwave after addition of ^{209}Po as an internal tracer. After plating onto high pure silver discs, polonium isotopes were counted by α-spectrometry using an Alpha Analyst Integrated Alpha Spectrometer equipped Passivated Implanted Planar Silicon detectors (CANBERRA). The concentrations of excess ^{210}Pb used to obtain the age models were determined as the difference between total ^{210}Pb and ^{226}Ra ($^{210}Pb_{supported}$). The concentrations of ^{226}Ra were determined for selected samples along each core by a low-background liquid scintillation counting method (Wallac 1220 Quantulus), adapted from Masqué et al. (2002). These concentrations were found to be in agreement with the concentrations of total ^{210}Pb at the depth below the excess ^{210}Pb horizons. The concentrations of ^{137}Cs in Core KGR-3 were determined by gamma ray spectrometry (Canberra Be3830) with a relative counting efficiency of 35% and an energy resolution of 1.8 keV (at 1,332 keV). Prior to the instrumental measurements, small shells were removed from the sediment samples. The activities of ^{137}Cs were determined from the gamma ray peak at 661.6 keV. These measurements were carried out at East China Normal University. The determination of ^{210}Pb and ^{137}Cs in Core CB-2 by gamma spectrometry were described in Liu et al. (2016).

2.3. Grain Size and TOC Measurements

Grain sizes were measured using a Malvern Mastersizer 2000F Laser Particle Sizer. Prior to the grain size measurements, the samples were pretreated using 10% H_2O_2 and 10% HCl to remove organic matter and carbonate, respectively, and then were dispersed in a 0.05% $(NaPO_3)_6$ solution to separate particles. TOC was measured using an elemental analyzer (Flash EA 1112 Thermo). Prior to the TOC measurements, the samples were freeze-dried, homogenized by grinding and acidified by 1 M HCl. The acidified samples were then dried at ~60 °C under flushing filtered air, mixed with 1-ml Milli-Q water and freeze-dried again.

2.4. Chemical Analysis of Biomarker Proxies

Two phytoplankton biomarkers, brassicasterol and dinosterol, were chosen to assess diatom and dinoflagellate biomasses in this study. Detailed methods of extraction and instrumental analyses followed the previous publications (Xing et al., 2016; Yuan et al., 2018). Briefly, freeze-dried sediments were extracted by CH_2Cl_2/CH_3OH (3:1, *v*/v). The extracts were hydrolyzed with 6% KOH in CH_3OH. The neutral fraction was extracted with hexane and then separated into two fractions-hydrocarbon fraction and polar lipid fraction using silica gel chromatography. The polar lipid fraction (containing brassicasterol and dinosterol) was eluted with CH_2Cl_2/CH_3OH (95:5, v/v), and then was derivatized using N, O-bis (trimethylsily)-trifluoroacetamide (BSTFA). The biomarker contents were determined by GC (Agilent 7890 A) with an FID detector and an HP-1 column (50 m × 0.32 μm × 0.17 μm). Both absolute content and TOC normalized content (e.g., nanogram of biomarker per gram of TOC in sediment) of biomarkers have been used as proxies for phytoplankton biomass (Xing et al., 2016; Zhao et al., 2006; Zimmerman & Canuel, 2000). In view of the possible preservation effect, our interpretations were based on the TOC normalized content of biomarkers.

2.5. Climatic Data Source and Statistical Analysis

The SST data were extracted from the extended reconstruction of SST data set (ERSST). They cover the sea area between 13–19°S and 121–127°E and the time period between 1930 and 2015 (http://apdrc.soest.hawaii.edu/; Smith et al., 2008). The rainfall data are from the Australian Bureau of Meteorology (http://www.bom.gov.au/). They are calculated from the averages of 11 rainfall stations covering the area of Kimberley coasts (Figures S1 in the supporting information) and the time period of 1930–2015. We consider the IPO a dominant climatic mode for interdecadal variability in north-western Australia (Salinger et al., 2016; Wainwright

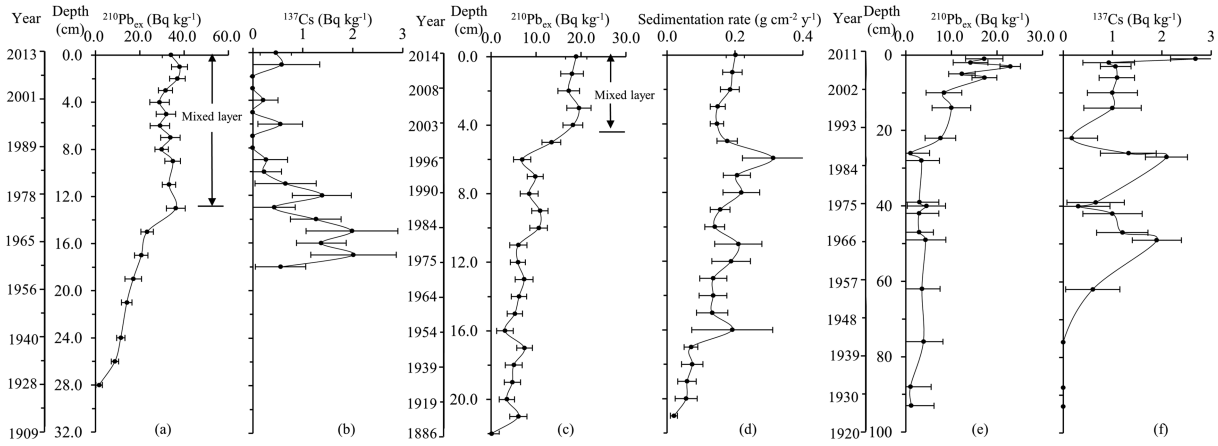

Figure 2. Profiles of a $^{210}Pb_{ex}$ and b ^{137}Cs at Core KGR-3, c $^{210}Pb_{ex}$ and d sedimentation rates at Core Broome-2, and e $^{210}Pb_{ex}$ and f ^{137}Cs at Core CB-2 (Liu et al., 2016; the error bars denote standard error).

et al., 2008). IPO values are obtained from KNMI Climate Explorer (http://climexp.knmi.nl/) calculated based on Hadley Centre sea ice and SST data (1930–2015) for understanding the interdecadal variability in north-western Australia.

The magnitude of the shift changes of phytoplankton biomarkers over time is assessed using the sequential *t* test analysis of regime shifts (STARS; Rodionov, 2004; Rodionov & Overland, 2005). The STARS algorithm is converted to VBA for Excel, which is available at the website (www.BeringClimate.noaa.gov). It uses a *t* test analysis to determine whether sequential records in a time series represent statistically significant departures from mean values observed during the preceding period of a predetermined duration. After the shift point is established, the value of the regime shift index (RSI) represents a cumulative sum of the normalized anomalies, which indicates the shift magnitude. The cut-off length (l) is set to 10 years, and the probability level to alpha = 0.05, representing a significant regime shift.

Interpolation analysis use Origin 8.0 software (mathematics: interpolate) to reduce asynchronous errors caused by the different sedimentation rates. Principle component analysis (PCA) use SPSS 16 (Statistical Package for the Social Sciences Inc.) to concentrate most of the variance of the large data set into a small number of interpretable patterns of variability in phytoplankton records. PCA analysis is based on the correlation matrix, which normalizes the data by the mean and standard deviation for each record. We used three types of outputs generated by PCA analysis: principal components (also called scores), eigenvectors (also termed loadings), and eigenvalues. The scores represent the temporal variability of extracted patterns. The loadings are used to illustrate the correlation between each record and principal component. The eigenvalues determine the fraction of total variance explained by each principal component.

3. Results

3.1. Chronology

The relatively constant values of $^{210}Pb_{ex}$ in the upper 14 cm of Core KGR-3 suggested the presence of a mixed layer, overlying a decreasing trend between 14 and 28 cm (Figure 2(a)). The CF:CS model (Constant Flux Constant Sedimentation; Krishnaswamy et al., 1971) was applied below the mixed layer for the 14- to 28-cm section, obtaining an average sedimentation rate of 0.14 ± 0.02 g·cm^{-2}·year^{-1} (or 3.0 ± 0.3 mm/year). This sedimentation rate would have led to the accumulation of the upper 32 cm of sediments between 1909 and 2013. However, given the relatively large part of the core that is mixed, the ^{137}Cs concentrations were measured to further confirm the ^{210}Pb chronology (Figure 2(b)). The first depth at which ^{137}Cs was detected was at 18–19 cm, and a relative maximum was present between 15 and 17 cm. This was in good agreement with the ^{210}Pb-derived chronology since ^{137}Cs was first introduced into the environment in 1954 and peaked in 1964 (Amos et al., 2009). The concentrations of $^{210}Pb_{ex}$ in Core Broome-2 (Figure 2(c)) indicated that the upper 5 cm were also mixed and steadily decrease thereafter and down to

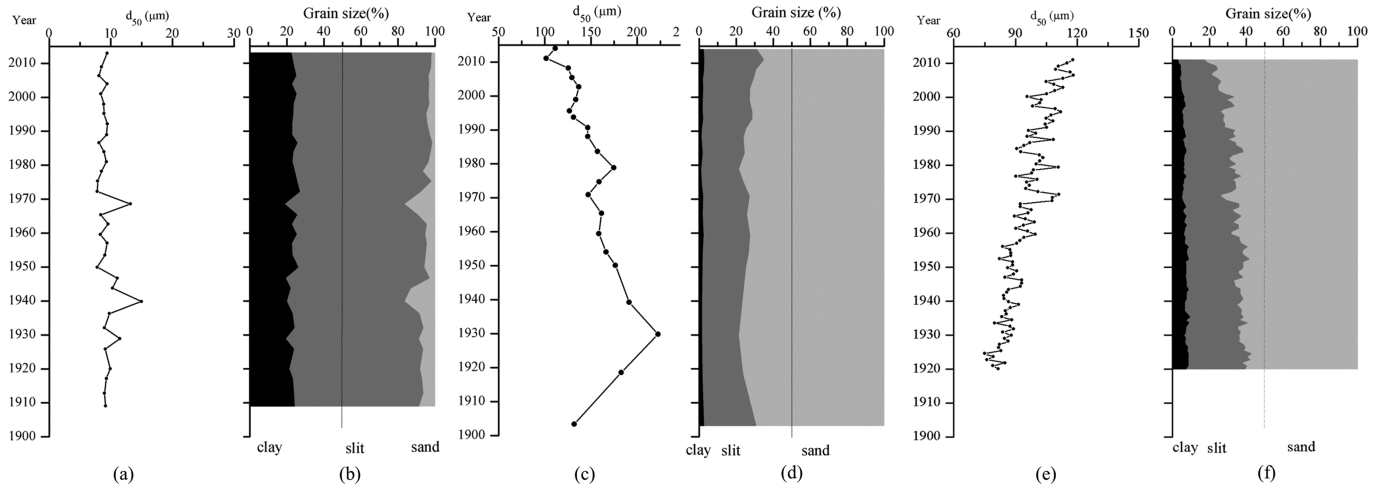

Figure 3. Profiles of grain sizes at (a and b) Core KGR-3, (c and d) Core Broome-2, and (e and f) Core CB-2 (Liu et al., 2016), showing median values (d_{50}) and the proportions of clay, silt, and sand.

22 cm. The application of the Constant Rate of Supply model (Appleby & Oldfield, 1978) allowed obtaining an age model for this core, with an average sedimentation rate of 0.16 ± 0.03 g·cm^{-2}·year^{-1} (or 2.5 ± 0.5 mm/year). For Core CB-2, the ^{210}Pb and ^{137}Cs dating was previously published (Figures 2(e) and 2(f)), and the application of CIC model generated an average sedimentation rate of 11.1 mm/year (Liu et al., 2016).

3.2. Grain Size Records

In Core KGR-3, the median grain size (d_{50}) showed little variation, with a range of 8–15 μm (Figure 3(a)), consisting of sand (mean of 6%), silt (mean of 71%), and clay (mean of 2%; Figure 3(b)). In Core Broome-2, the d_{50} became finer over time, varying from 101 to 223 μm (Figure 3(c)), consisting of sand (mean of 73%), silt (mean of 25%), and clay (mean of 2%; Figure 3(d)). The grain size data in Core CB-2 were reported previously by Liu et al. (2016). The median grain size varies from 75 to 118 μm (Figure 3(e)), and grain size became coarser over time (Figure 3(f)). In comparison, the grain sizes of Core KGR-3 were much finer than that of Cores Broome-2 and Core CB-2.

3.3. Biomarker Records

In Core KGR-3, TOC normalized brassicasterol and dinosterol contents indicated two periods according to the STARS analysis (Figures 4(a) and 4(b)): (1) During the first period (1909–1954), brassicasterol and dinosterol contents were relatively lower, averaging 11.0 and 17.0 μg/g TOC, respectively. (2) During the second period (1954–2013), brassicasterol and dinosterol contents were relatively higher. Brassicasterol contents increased gradually with two significant shifts (RSI: 1.6 and 0.3; average: 20.1 and 25.7 μg/g TOC, respectively). Dinosterol contents showed a rapid increase during 1954–1975 (RSI: 1.4; average: 26.6 μg/g TOC) and a small decrease during 1975–2013 (RSI: −0.4; average: 21.9 μg/g TOC).

In Core Broome-2, TOC normalized brassicasterol and dinosterol contents showed an increasing period after 1978 (Figures 4(c) and 4(d)). Brassicasterol contents showed two significant increasing shifts in 1978 and 1997, respectively, according to the STARS analysis (RSI: 0.6 and 0.6; Figure 4(c)). The averaged contents during 1903–1978, 1978–1997, and 1997–2015 were 23.0, 36.6, and 50.8 μg/g TOC, respectively. The averaged dinosterol contents before and after 1978 (RSI: 0.2; Figure 4(d)) were 54.2 and 70.4 μg/g TOC, respectively.

In Core CB-2, TOC normalized brassicasterol and dinosterol contents also showed an increasing trend (Figures 4(e) and 4(f)). According to the STARS analysis, brassicasterol contents indicated two significant periods (RSI: 1.0 and 2.8; Figure 4(e)), with lower values during 1920–1997 (average: 8.7 μg/g TOC) and higher values during 1997–2011 (average: 35.8 μg/g TOC). Dinosterol contents started to increase after the 1950s, and significant shifts occurred after 1982 (RSI: 0.8 and 1.2; Figure 4(f)), with lower values during 1920–1982 (average: 23.8 μg/g TOC) and higher values during 1982–2011 (average: 46.8 μg/g TOC).

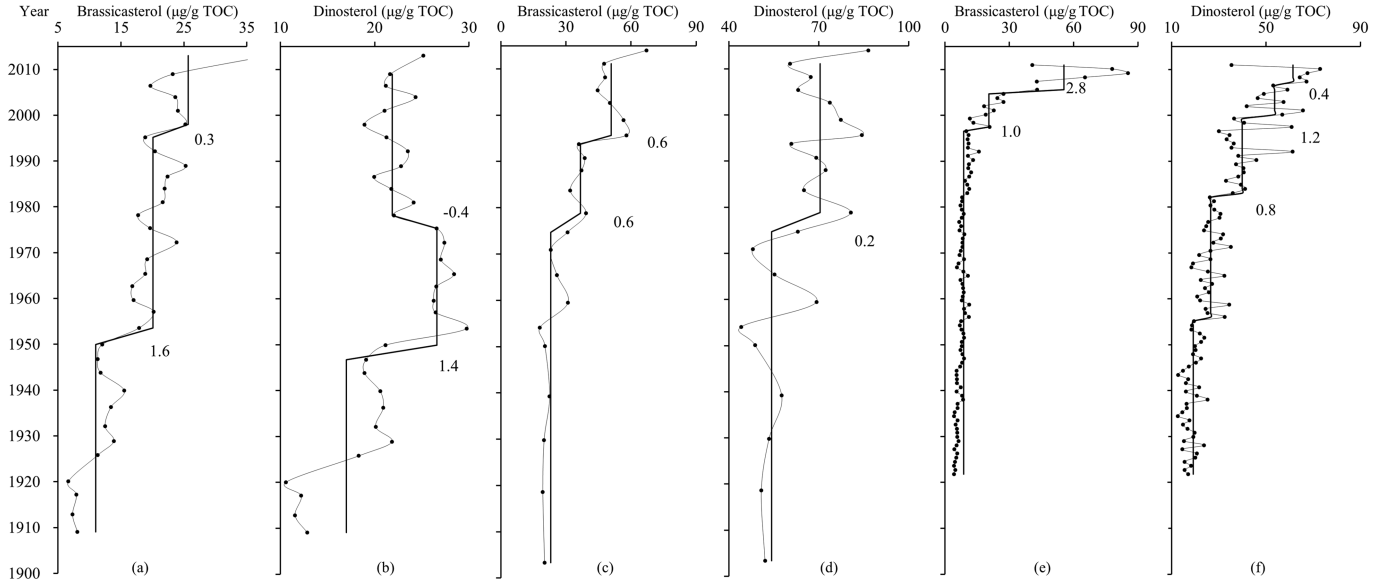

Figure 4. Profiles of TOC normalized brassicasterol and dinosterol contents in (a and b) Core KGR-3, (c and d) Core Broome-2, and (e and f) Core CB-2 (Yuan et al., 2018). The solid lines show shift trends assessed by sequential *t* test analysis of regime shift and numbers are regime shift index.

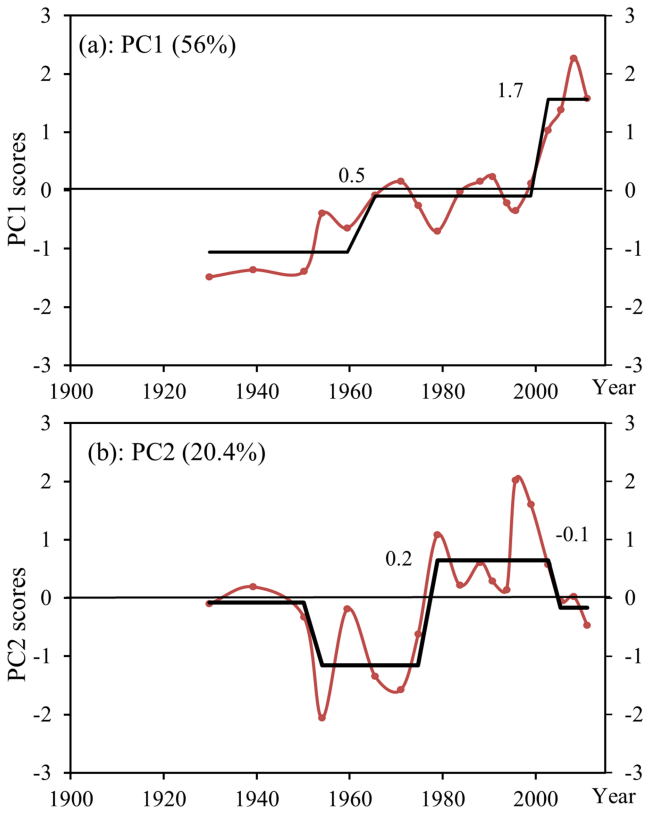

Figure 5. Principal component (PC) scores (red lines) constructed from the diatoms and dinoflagellates records in North-Western Australia (a: PC1 and b: PC2). The black lines show shift trends assessed by sequential *t* test analysis of regime shift and numbers are regime shift index.

In a summary, biomarker records at three locations showed a distinct increase, albeit their shifting time, frequency, and magnitude were different.

3.4. Principal Variation Patterns in Phytoplankton Biomass

To extract the most common signals of phytoplankton variations, PCA analysis was performed on the dataset containing the TOC normalized brassicasterol and dinosterol contents in cores KGR-3, CB-2, and Broome-2. Prior to PCA analysis, interpolation analysis generated an average time scale of ~4 years for all the records. This data processing may smooth the variability within 4 years. However, this bias can be ignored, as the time scale in this study focused on interdecadal oscillations, which were much longer than 4 years. Eigenvalues indicated that the first two principal components, accounting for 56% and 20.4% of the total variance, were meaningful (Figure 5). The first principal component (PC1) displayed a gradually increasing trend, with two significant shifts in 1965 and 1999 (Figure 5(a)). High loadings ($r > 0.5$) on PC1 were related to the brassicasterol records at the three locations and the dinosterol record in Core CB-2 (Figure 6). In contrast, the second principal component (PC2) displayed oscillations, with one increasing shift at 1979 and one decreasing shift at 2002 (Figure 5(b)). High loadings ($r > 0.5$) on PC2 were associated with the brassicasterol and dinosterol records in Core Broome-2 (Figure 6). Considering the mixed layer in Core KGR-3 (upper 14 cm), a test of using PCA analysis without the data in Core KGR-3 also generated two similar PCs. Although these two PCs were different in their accounted total variance, it did not change their correlations with instrumental climatological data.

The scores of PC1 and PC2 were further compared with the trends of regional SST, rainfall, and IPO during 1930–2015 (Figure 7). The increasing pattern of PC1 was broadly consistent with regional SST and rainfall records (Figures 7(a) and 7(b)), with significant correlations (Table 1;

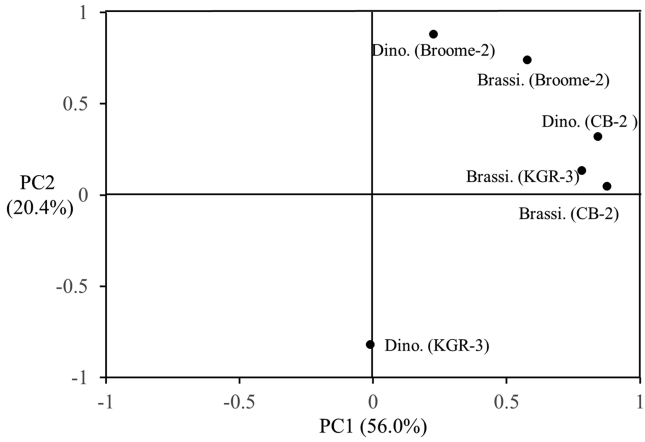

Figure 6. Plots of brassicasterol (brassi.) and dinosterol (dino.) loadings on PC1 and PC2 based on principal component analysis.

Pearson correlation coefficients were 0.60 for SST and 0.57 for rainfall, $p < 0.05$). In a comparison, brassicasterol records showed more significant correlations with regional rainfall than dinosterol records (Table 1). The pattern of PC2 corresponded well with shifts in IPO between warm and cool phases (Figure 7(c)), with a Pearson correlation coefficient of 0.48 (Table 1).

4. Discussion

Since the 1950s, diatom and dinoflagellate biomasses showed a 1.5–3 times increase and the increase of diatoms overwhelmed dinoflagellates, although the shifting patterns in the three bays are not always coincident (Figure 4). The overall trend supports the field observations between the 1960s and 1990s in northern Australia, with a twofold increase in primary productivity (Furnas & Carpenter, 2016). The results showed that the increased biomasses were significantly correlated with increased SST and rainfall. Moreover, phytoplankton biomass also displayed interdecadal oscillations, coinciding with the shifts of IPO in warm and cold phases. In the discussion below, the possible mechanisms of SST, rainfall, and IPO acting on the phytoplankton assemblages were discussed for better understanding the results.

4.1. SST and Rainfall

Modeling studies predict that ocean warming will result in a reduction in marine primary productivity (up to 20%) throughout the twenty-first century (Steinacher et al., 2010), because rising temperatures challenge the limit of thermal tolerance of phytoplankton and enhance stratification, which consequently suppresses vertical mixing and reduces the nutrient supply to the phytoplankton living in the upper ocean (Lewandowska et al., 2014). However, the effects of stratification are not as apparent in shallow coastal waters, due to strong mixing (Cloern & Jassby, 2010); this is particularly true on the Kimberley coast, with the second largest tidal system in the world (Holloway, 1983; Wolanski & Spagnol, 2003). Thus, we need to consider the physiological responses of phytoplankton to rising temperatures. There is growing evidence to show fast adaptation of phytoplankton to ocean warming, particularly for tropical species (Jin & Agustí, 2018; Padfield et al., 2016; Schaum et al., 2017). The short generation times and high population density of phytoplankton make it possible for them to undergo evolutionary responses to rising temperatures after 80–450 generations (Padfield et al., 2016). For example, culture experiments showed that diatoms are less sensitive to increasing temperature than other phytoplankton groups, but two tropical species adapted to higher temperatures after 200–600 generations, and also increased their optimal temperature and maximum growth rate (Jin & Agustí, 2018). The mechanism of evolutionary adaptation to warming helps to explain why rising temperature did not decrease the biomasses of diatoms and dinoflagellates in the Kimberley coast and diatoms increased faster than dinoflagellates.

Rising temperatures force increases in tropical cyclone intensity and heavy rainfall (Diffenbaugh et al., 2018; Sobel et al., 2016). North-western Australia is one of the world's tropical cyclone hot spots, and much of the increased rainfall over recent decades is attributed to the contribution of tropical cyclones (Lavender & Abbs, 2013). Tropical cyclones not only increase rainfall but also enhance vertical mixing of seawater and sediment resuspension in coastal waters. These dynamic processes improve the nutrient supply and accelerate metabolic capability of phytoplankton and turnover rate of bacteria working on organic matter (McKinnon et al., 2003). Phytoplankton living in tropical oligotrophic water is sensitive to nutrient enhancement (Cloern & Jassby, 2010). Modeling results suggested that the tropical cyclone-induced phytoplankton blooms in north-western Australia could contribute to 20% of annual primary production (Menkes et al., 2016). The shift changes of diatoms and dinoflagellates in the three locations were asynchronous after the 1970s, which might be related to their different geographic and hydrologic conditions. For example, Core CB-2 located in Cygnet Bay was collected close to Fitzroy River; thus, it could be more sensitive to rainfall changes due to the direct input of fluvial materials. That also explained the fact that Core CB-2 had much higher sedimentation rate than Core Broome-2 and KGR-3. Spatial grain size pattern implies that the sites of Core CB-2 and

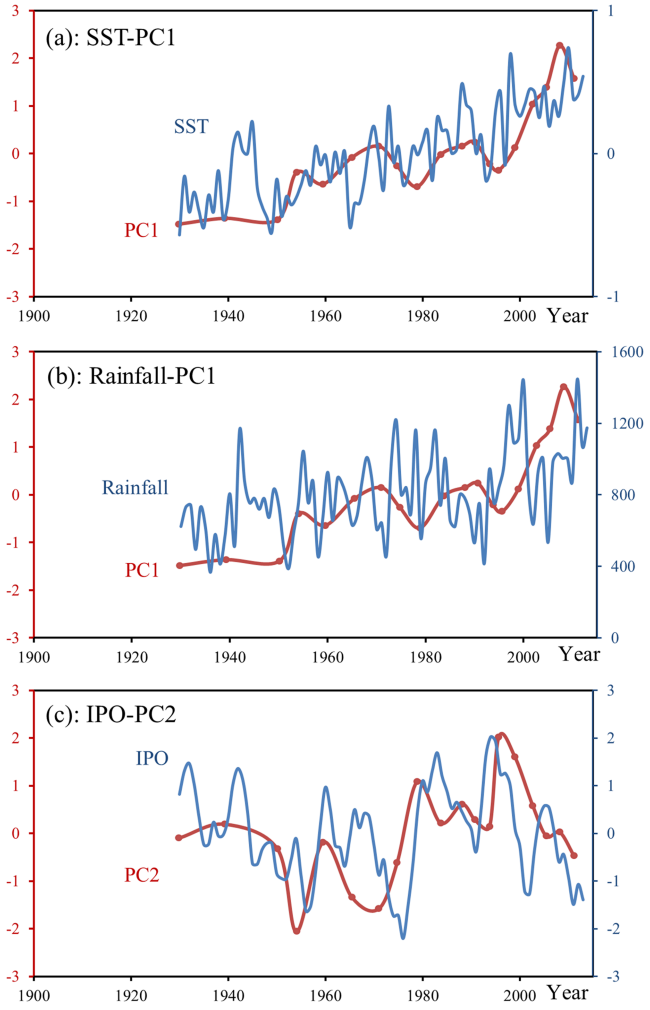

Figure 7. Comparisons of principal component (PC) scores (red lines), SST, rainfall, and IPO (blue lines). a: PC1 and regional SST; b: PC1 and regional rainfall; c: PC2 and IPO. Regional SST and rainfall were from the extended reconstruction of SST data set (ERSST, http://apdrc.soest.hawaii.edu/) and from the Australian Bureau of Meteorology (http://www.bom.gov.au/), respectively; IPO records were calculated based on HadISST data (http://climexp.knmi.nl/).

Table 1
Pearson Correlation Coefficients

Phytoplankton records		Regional SST	Regional rainfall	IPO
PC1		0.60*	0.57*	−0.27
PC2		0.36	0.21	0.48
Broome-2	Brassicasterol	0.64*	0.59*	0.14
	Dinosterol	0.58*	0.28	0.29
CB-2	Brassicasterol	0.47*	0.38*	−0.16
	Dinosterol	0.60*	0.35*	−0.06
KGR-3	Brassicasterol	0.71*	0.40*	−0.11
	Dinosterol	0.33	0.05	−0.12

*Correlation is significant at $p < 0.05$

Broome-2 have experienced more energetic conditions capable of transporting larger particle sizes. Moreover, a coarser trend of grain size over time was found in Core CB-2, possibly caused by the increased rainfall and tropical cyclone-induced flood events accompanied by more coarse loads.

In addition, diatoms and dinoflagellates have different ecological preferences; for example, diatoms prefer lower salinity and temperature and cannot live without silicate required for frustule synthesis; dinoflagellates favor warmer temperature and higher salinity and need not use silicate in their life cycle (Irwin et al., 2012; Margalef, 1978; Mutshinda et al., 2013). Increased rainfall not only buffers salinity but also brings silicate, because riverine inputs are the most important source of dissolved silicate in the ocean (Tréguer & De La Rocha, 2013). Therefore, diatoms obtain greater benefit than dinoflagellates from increasing rainfall. Field observations on the Kimberley coast during 2010 also showed that the pigment proportion of diatoms in shallow water (<50 m) was much higher than dinoflagellates (Thompson & Bonham, 2011). Another example is Tropical Cyclone Bobby in February 1995, when diatom production in coastal waters of northwest Australia increased twofold after the cyclone (Condie et al., 2009). This information helps to explain the fast increase of diatom biomass in the sediment cores after the 1990s (Figure 4) and why diatoms show better correlations with increased rainfall than dinoflagellates (Table 1).

4.2. IPO

IPO is a basin-scale temperature pattern in the tropical Pacific (Power et al., 1999; Zhang et al., 1997). It strongly influences the ITF transport from the Western Pacific toward the shelf of northwest Australia on decadal scales (Feng et al., 2011; Wainwright et al., 2008), and consequently, the intensity of the ITF impacts the water exchange between shelf and coast (Armbrecht et al., 2015; McKinnon et al., 2015). In this study, the IPO-like pattern (PC2) explained 20.6% of the total variance in the phytoplankton records (Figure 7(c)). Previous field observations (e.g., North West Cape and Darwin Harbor) showed that nutrient inputs transporting from deep water through enhanced upwelling have a significant contribution to the coastal nutrient budget, which can further adjust phytoplankton productivity (Burford et al., 2008; Furnas, 2007). Therefore, the coupling correlation between IPO and phytoplankton variations could be determined through the ocean-coast interaction via the intensity of the ITF transport (Furnas, 2007).

During the warm phase of IPO, the transport of the ITF from the Western Pacific is weaker (Feng et al., 2011; Wainwright et al., 2008). Weak ITF corresponding to strong coastal upwelling can enhance the nutrient transport from deep waters and consequently form a positive influence on the coastal phytoplankton (Furnas, 2007; Thompson et al., 2015). Conversely, the cold phase of IPO is associated with stronger transport of ITF from the Western Pacific. Strong ITF can suppress the coastal upwelling and reduce nutrient supply from deep waters to coastal waters (Furnas, 2007). IPO was in a cold phase during 1945 to 1979, switched to a warm phase from 1979 to 1999 and then once again to a cold phase where it remained to present (Figure 7(c)). In this study, dinoflagellates indicate a more significant response to IPO phases than diatoms, via a decline or slowing down their increasing biomass trend after IPO shifted to cold phase at 1999 (Figure 4).

Moreover, dinoflagellate records in the three bays show higher loadings on PC2 than diatom records (Figure 6). This might be related to different environmental tolerance between dinoflagellates and diatoms. In a comparison, diatoms are tolerant of a wider range of salinity and temperature than dinoflagellates, which can help them better to adapt the variations in salinity and temperature caused by strong transport of the ITF during the cold phase of IPO.

5. Conclusions

In summary, phytoplankton productivity in the Kimberley coast reconstructed by biomarkers revealed both overall increasing trends and interdecadal oscillations, possibly driven by rising SST and rainfall, and shifts in warm and cold phases of IPO. The IPCC 2018 report proposed that the impacts of global warming are likely to occur between 2030 and 2052. Climatic models in Australia predicted increasing SST and intense tropical cyclones around north-western Australia in the future (Lavender & Walsh, 2011; Lough & Hobday, 2011; Poloczanska et al., 2007; Ren & Leslie, 2015). When considering the low-pass-filtered index, major IPO eras generally persist 20 to 30 years and it appears to terminate the current cold phase and turn to warm phase (Mantua et al., 1997). Therefore, we make an empirical prediction that, unlike other places around the world, the sharp decline of phytoplankton productivity in north-western Australia might not occur in coming decades.

Acknowledgments
The study is funded by Natural Science Foundations of China (41876127, 41641048, and 41630966), Generalitat de Catalunya (MERS 2017 SGR-1588), the Australian Research Council LIEF Project (LE170100219), and the Western Australian Marine Sciences Institution. We thank the crews of the RV Solander (Australian Institute of Marine Science) and James McLaughlin for assistance in taking the cores, Joanna Strzelecki assisted with core sectioning and freeze-drying sediments, Yajun Peng and Yujue Wang for Grain Size and TOC analysis, and Hailong Zhang and Li Li for technical support. This work contributes to the ICTA Unit of Excellence (MinECo, MDM2015-0552). The data used here are available in the Pangaea online database (https://doi.pangaea.de/10.1594/PANGAEA.911180).

References

Amos, K. J., Croke, J. C., Timmers, H., Owens, P. N., & Thompson, C. (2009). The application of caesium-137 measurements to investigate floodplain deposition in a large semi-arid catchment in Queensland, Australia: A low-fallout environment. *Earth Surface Processes and Landforms*, *34*(4), 515–529. https://doi.org/10.1002/esp.1749

Appleby, P., & Oldfield, F. (1978). The calculation of lead-210 dates assuming a constant rate of supply of unsupported ^{210}Pb to the sediment. *Catena*, *5*(1), 1–8. https://doi.org/10.1016/S0341-8162(78)80002-2

Armbrecht, L. H., Thompson, P. A., Wright, S. W., Schaeffer, A., Roughan, M., Henderiks, J., & Armand, L. K. (2015). Comparison of the cross-shelf phytoplankton distribution of two oceanographically distinct regions off Australia. *Journal of Marine Systems*, *148*, 26–38. https://doi.org/10.1016/j.jmarsys.2015.02.002

Behrenfeld, M. J., O'Malley, R. T., Siegel, D. A., McClain, C. R., Sarmiento, J. L., Feldman, G. C., et al. (2006). Climate-driven trends in contemporary ocean productivity. *Nature*, *444*(7120), 752–755. https://doi.org/10.1038/nature05317

Boyce, D. G., & Worm, B. (2015). Patterns and ecological implications of historical marine phytoplankton change. *Marine Ecology Progress Series*, *534*, 251–272. https://doi.org/10.3354/meps11411

Burford, M. A., Alongi, D. M., McKinnon, A. D., & Trott, L. A. (2008). Primary production and nutrients in a tropical macrotidal estuary, Darwin harbour, Australia. *Estuarine, Coastal and Shelf Science*, *79*(3), 440–448. https://doi.org/10.1016/j.ecss.2008.04.018

Burns, K. A., Volkman, J. K., Cavanagh, J.-A., & Brinkman, D. (2003). Lipids as biomarkers for carbon cycling on the northwest shelf of Australia: Results from a sediment trap study. *Marine Chemistry*, *80*(2), 103–128. https://doi.org/10.1016/S0304-4203(02)00099-3

Cloern, J. E., & Jassby, A. D. (2010). Patterns and scales of phytoplankton variability in estuarine-coastal ecosystems. *Estuaries and Coasts*, *33*(2), 230–241. https://doi.org/10.1007/s12237-009-9195-3

Condie, S., Herzfeld, M., Margvelashvili, N., & Andrewartha, J. (2009). Modeling the physical and biogeochemical response of a marine shelf system to a tropical cyclone. *Geophysical Research Letters*, *36*(22), L22603. https://doi.org/10.1029/2009GL039563

Diffenbaugh, N. S., Singh, D., & Mankin, J. S. (2018). Unprecedented climate events: Historical changes, aspirational targets, and national commitments. *Science Advances*, *4*(2), eaao3354. https://doi.org/10.1126/sciadv.aao3354

Feng, M., Böning, C., Biastoch, A., Behrens, E., Weller, E., & Masumoto, Y. (2011). The reversal of the multi-decadal trends of the equatorial Pacific easterly winds, and the Indonesian Throughflow and Leeuwin current transports. *Geophysical Research Letters*, *38*, L11604. https://doi.org/10.1029/2011GL047291

Field, C. B., Behrenfeld, M. J., Randerson, J. T., & Falkowski, P. (1998). Primary production of the biosphere: Integrating terrestrial and oceanic components. *Science*, *281*(5374), 237–240. https://doi.org/10.1126/science.281.5374.237

Finkel, Z. V., Beardall, J., Flynn, K. J., Quigg, A., Rees, T. A. V., & Raven, J. A. (2010). Phytoplankton in a changing world: Cell size and elemental stoichiometry. *Journal of Plankton Research*, *32*(1), 119–137. https://doi.org/10.1093/plankt/fbp098

Furnas, M. J. (2007). Intra-seasonal and inter-annual variations in phytoplankton biomass, primary production and bacterial production at north west cape, Western Australia: Links to the 1997-1998 El Niño event. *Continental Shelf Research*, *27*, 958–980. https://doi.org/10.1016/j.csr.2007.01.002

Furnas, M. J., & Carpenter, E. J. (2016). Primary production in the tropical continental shelf seas bordering northern Australia. *Continental Shelf Research*, *129*, 33–48. https://doi.org/10.1016/j.csr.2016.06.006

Halpern, B. S., Walbridge, S., Selkoe, K. A., Kappel, C. V., Micheli, F., D'Agrosa, C., et al. (2008). A global map of human impact on marine ecosystems. *Science*, *319*(5865), 948–952. https://doi.org/10.1126/science.1149345

Hassim, M. E., & Walsh, K. J. (2008). Tropical cyclone trends in the Australian region. *Geochemistry, Geophysics, Geosystems*, *9*(7), 1–17. https://doi.org/10.1029/2007GC001804

Hays, G. C., Richardson, A. J., & Robinson, C. (2005). Climate change and marine plankton. *Trends in Ecology & Evolution*, *20*(6), 337–344. https://doi.org/10.1016/j.tree.2005.03.004

Henson, S. A., Sarmiento, J. L., Dunne, J. P., Bopp, L., Lima, I. D., Doney, S. C., et al. (2010). Detection of anthropogenic climate change in satellite records of ocean chlorophyll and productivity. *Biogeosciences*, *7*, 621–640. https://doi.org/10.5194/bg-7-621-2010

Holloway, P. (1983). Tides on the Australian north-west shelf. *Marine and Freshwater Research*, *34*(1), 213–230. https://doi.org/10.1016/0198-0254(83)96398-7

Holloway, P., & Nye, H. (1985). Leeuwin current and wind distributions on the southern part of the Australian north west shelf between January 1982 and July 1983. *Marine and Freshwater Research*, *36*(2), 123–137. https://doi.org/10.1071/mf9850123

Irwin, A. J., Nelles, A. M., & Finkel, Z. V. (2012). Phytoplankton niches estimated from field data. *Limnology and Oceanography*, *57*(3), 787–797. https://doi.org/10.4319/lo.2012.57.3.0787

Jin, P., & Agustí, S. (2018). Fast adaptation of tropical diatoms to increased warming with trade-offs. *Scientific Reports*, *8*(1), 17,771. https://doi.org/10.1038/s41598-018-36091-y

Keesing, J. K. (2014). Marine biodiversity and ecosystem function in the King George River region of north-western Australia *Report*, 145 pp, CSIRO, Australia.

Keesing, J. K., Irvine, T. R., Alderslade, P., Clapin, G., Fromont, J., Hosie, A., et al. (2011). Marine benthic flora and fauna of Gourdon Bay and the Dampier peninsula in the Kimberley region of North-Western Australia. *Journal of the Royal Society of Western Australia*, *94*(2), 285–301.

Krishnaswamy, S., Lal, D., Martin, J. M., & Meybeck, M. (1971). Geochronology of lake sediments. *Earth and Planetary Science Letters*, *11*(1), 407–414. https://doi.org/10.1016/0012-821X(71)90202-0

Lavender, S. L., & Abbs, D. J. (2013). Trends in Australian rainfall: Contribution of tropical cyclones and closed lows. *Climate Dynamics*, *40*(1-2), 317–326. https://doi.org/10.1007/s00382-012-1566-y

Lavender, S. L., & Walsh, K. J. E. (2011). Dynamically downscaled simulations of Australian region tropical cyclones in current and future climates. *Geophysical Research Letters*, *38*(10), L10705. https://doi.org/10.1029/2011GL047499

Lewandowska, A. M., Boyce, D. G., Hofmann, M., Matthiessen, B., Sommer, U., & Worm, B. (2014). Effects of sea surface warming on marine plankton. *Ecology Letters*, *17*(5), 614–623. https://doi.org/10.1111/ele.12265

Liu, D., Peng, Y., Keesing, J. K., Wang, Y., & Richard, P. (2016). Paleo-ecological analyses to assess long-term environmental effects of pearl farming in Western Australia. *Marine Ecology Progress Series*, *552*, 145–158. https://doi.org/10.3354/meps11740

Lough, J. M. (2008). Shifting climate zones for Australia's tropical marine ecosystems. *Geophysical Research Letters*, *35*(14), L14708. https://doi.org/10.1029/2008GL034634

Lough, J. M., & Hobday, A. J. (2011). Projected climate change in Australian marine and freshwater environments. *Marine and Freshwater Research*, *62*(9), 1000–1014. https://doi.org/10.1071/MF10302

Mantua, N. J., Hare, S. R., Zhang, Y., Wallace, J. M., & Francis, R. C. (1997). A Pacific interdecadal climate oscillation with impacts on salmon production. *Bulletin of the American Meteorological Society*, *78*(6), 1069–1079. https://doi.org/10.1175/1520-0477(1997)078<1069:APICOW>2.0.CO;2

Margalef, R. (1978). Life-forms of phytoplankton as survival alternatives in an unstable environment. *Oceanologica Acta*, *1*(4), 493–509. https://doi.org/10.1016/0302-184X(78)90008-2

Martinez, E., Antoine, D., D'Ortenzio, F., & Gentili, B. (2009). Climate-driven basin-scale decadal oscillations of oceanic phytoplankton. *Science*, *326*(5957), 1253–1256. https://doi.org/10.1126/science.1177012

Masqué, P., Sanchez-Cabeza, J., Bruach, J., Palacios, E., & Canals, M. (2002). Balance and residence times of ^{210}Pb and ^{210}Po in surface waters of the northwestern Mediterranean Sea. *Continental Shelf Research*, *22*(15), 2127–2146. https://doi.org/10.1016/s0278-4343(02)00074-2

McKinnon, A., Duggan, S., Holliday, D., & Brinkman, R. (2015). Plankton community structure and connectivity in the Kimberley-browse region of NW Australia. *Estuarine, Coastal and Shelf Science*, *153*, 156–167. https://doi.org/10.1016/j.ecss.2014.11.006

McKinnon, A., Meekan, M., Carleton, J., Furnas, M., Duggan, S., & Skirving, W. (2003). Rapid changes in shelf waters and pelagic communities on the southern northwest shelf, Australia, following a tropical cyclone. *Continental Shelf Research*, *23*(1), 93–111. https://doi.org/10.1016/S0278-4343(02)00148-6

Menkes, C. E., Lengaigne, M., Lévy, M., Ethé, C., Bopp, L., Aumont, O., et al. (2016). Global impact of tropical cyclones on primary production. *Global Biogeochemical Cycles*, *30*(5), 767–786. https://doi.org/10.1002/2015GB005214

Meyers, G. (1996). Variation of Indonesian throughflow and the El Niño-southern oscillation. *Journal of Geophysical Research, Oceans*, *101*(C5), 12,255–12,263. https://doi.org/10.1029/95JC03729

Mutshinda, C. M., Finkel, Z. V., & Irwin, A. J. (2013). Which environmental factors control phytoplankton populations? A Bayesian variable selection approach. *Ecological Modelling*, *269*, 1–8. https://doi.org/10.1016/j.ecolmodel.2013.07.025

O'Donnell, A. J., Cook, E. R., Palmer, J. G., Turney, C. S., Page, G. F., & Grierson, P. F. (2015). Tree rings show recent high summer-autumn precipitation in Northwest Australia is unprecedented within the last two centuries. *PLoS ONE*, *10*(6), e0128533. https://doi.org/10.1371/journal.pone.0128533

Padfield, D., Yvon-Durocher, G., Buckling, A., Jennings, S., Yvon-Durocher, G., & Hillebrand, H. (2016). Rapid evolution of metabolic traits explains thermal adaptation in phytoplankton. *Ecology Letters*, *19*(2), 133–142. https://doi.org/10.1111/ele.12545

Paerl, H. W., & Scott, J. T. (2010). Throwing fuel on the fire: Synergistic effects of excessive nitrogen inputs and global warming on harmful algal blooms. *Environmental Science & Technology*, *44*(20), 7756–7758. https://doi.org/10.1021/es102665e

Poloczanska, E. S., Babcock, R. C., Butler, A., Hobday, A. J., Hoegh-Guldberg, O., Kunz, T. J., et al. (2007). Climate change and Australian marine life. *Oceanography and Marine Biology*, *45*, 407–478. https://doi.org/10.1201/9781420050943.ch8

Power, S., Casey, T., Folland, C., Colman, A., & Mehta, V. (1999). Inter-decadal modulation of the impact of ENSO on Australia. *Climate Dynamics*, *15*(5), 319–324. https://doi.org/10.1007/s003820050284

Ren, D., & Leslie, L. M. (2015). Changes in tropical cyclone activity over Northwest Western Australia in the past 50 years and a view of the future 50 years. *Earth Interactions*, *19*(15), 1–24. https://doi.org/10.1175/ei-d-14-0006.1

Rodionov, S. N. (2004). A sequential algorithm for testing climate regime shifts. *Geophysical Research Letters*, *31*(9), L09204. https://doi.org/10.1029/2004gl019448

Rodionov, S. N., & Overland, J. E. (2005). Application of a sequential regime shift detection method to the Bering Sea ecosystem. *ICES Journal of Marine Science*, *62*(3), 328–332. https://doi.org/10.1016/j.icesjms.2005.01.013

Salinger, J., Hobday, A. J., Matear, R. J., O'Kane, T. J., Risbey, J. S., Eveson, J. P., et al. (2016). Decadal-scale forecasting of climate drivers for marine applications. *Advances in Marine Biology*, *74*, 1–68. https://doi.org/10.1016/bs.amb.2016.04.002

Sánchez-Cabeza, J., Masqué, P., & Ani-Ragolta, I. (1998). ^{210}Pb and ^{210}Po analysis in sediments and soils by microwave acid digestion. *Journal of Radioanalytical and Nuclear Chemistry*, *227*(1–2), 19–22. https://doi.org/10.1007/BF02386425

Schaum, C. E., Barton, S., Bestion, E., Buckling, A., Garcia-Carreras, B., Lopez, P., et al. (2017). Adaptation of phytoplankton to a decade of experimental warming linked to increased photosynthesis. *Nature Ecology and Evolution*, *1*(4), 94. https://doi.org/10.1038/s41559-017-0094

Schlüter, L., Kai, T. L., Gutowska, M. A., Gröger, J. P., Riebesell, U., & Reusch, T. B. H. (2014). Adaptation of a globally important coccolithophore to ocean warming and acidification. *Nature Climate Change*, *4*(11), 1024–1030. https://doi.org/10.1038/nclimate2379

Smith, T. M., Reynolds, R. W., Peterson, T. C., & Lawrimore, J. (2008). Improvements to NOAA's historical merged land-ocean surface temperature analysis (1880-2006). *Journal of Climate*, *21*(10), 2283–2296. https://doi.org/10.1175/2007JCLI2100.1

Smittenberg, R., Pancost, R., Hopmans, E., Paetzel, M., & Damsté, J. S. (2004). A 400-year record of environmental change in an euxinic fjord as revealed by the sedimentary biomarker record. *Palaeogeography, Palaeoclimatology, Palaeoecology*, *202*(3), 331–351. https://doi.org/10.1016/S0031-0182(03)00642-4

Sobel, A. H., Camargo, S. J., Hall, T. M., Lee, C. Y., Tippett, M. K., & Wing, A. A. (2016). Human influence on tropical cyclone intensity. *Science*, *353*(6296), 242–246. https://doi.org/10.1126/science.aaf6574

Steinacher, M., Joos, F., Frolicher, T., Bopp, L., Cadule, P., Cocco, V., et al. (2010). Projected 21st century decrease in marine productivity: A multi-model analysis. *Biogeosciences*, *7*(3), 979–1005. https://doi.org/10.5194/bg-7-979-2010

Thompson, P. A., & Bonham, P. (2011). New insights into the Kimberley phytoplankton and their ecology. *Journal of the Royal Society of Western Australia*, *94*, 161–170.

Thompson, P. A., Bonham, P., Thomson, P., Rochester, W., Doblin, M. A., Waite, A. M., et al. (2015). Climate variability drives plankton community composition changes: The 2010–2011 El Niño to La Niña transition around Australia. *Journal of Plankton Research*, *37*(5), 1–19. https://doi.org/10.1093/plankt/fbv069

Tréguer, P., & De La Rocha, C. (2013). The world ocean silica cycle. *Annual Review of Marine Science*, *5*(5), 477–501.

Volkman, J. K., Barrett, S. M., Blackburn, S. I., Mansour, M. P., Sikes, E. L., & Gelin, F. (1998). Microalgal biomarkers: A review of recent research developments. *Organic Geochemistry*, *29*(5–7), 1163–1179. https://doi.org/10.1016/S0146-6380(98)00062-X

Wainwright, L., Meyers, G., Wijffels, S., & Pigot, L. (2008). Change in the Indonesian Throughflow with the climatic shift of 1976/77. *Geophysical Research Letters*, *35*(3), L03604. https://doi.org/10.1029/2007GL031911

Wilson, B. (2013). *The Biogeography of the Australian North West Shelf: Environmental Change and life's Response*. Burlington, MA, USA: Elsevier.

Woinarski, J., Mackey, B., Nix, H., & Traill, B. (2007). *The Nature of Northern Australia: It's natural values, ecological processes and future prospects*. Canberra, Australia: ANU e Press.

Wolanski, E., & Spagnol, S. (2003). Dynamics of the turbidity maximum in king sound, tropical Western Australia. *Estuarine, Coastal and Shelf Science*, *56*(5), 877–890. https://doi.org/10.1016/s0272-7714(02)00214-7

Xing, L., Zhao, M., Zhang, T., Yu, M., Duan, S., Zhang, R., et al. (2016). Ecosystem responses to anthropogenic and natural forcing over the last 100 years in the coastal areas of the East China Sea. *The Holocene*, *26*(1), 1–9. https://doi.org/10.1177/0959683615618248

Yuan, Z., Liu, D., Keesing, J. K., Zhao, M., Guo, S., Peng, Y., & Zhang, H. (2018). Paleoecological evidence for decadal increase in phytoplankton biomass off northwestern Australia in response to climate change. *Ecology and Evolution*, *8*(4), 2097–2107. https://doi.org/10.1002/ece3.3836

Yvon-Durocher, G., Dossena, M., Trimmer, M., Woodward, G., & Allen, A. P. (2015). Temperature and the biogeography of algal stoichiometry. *Global Ecology and Biogeography*, *24*(5), 562–570. https://doi.org/10.1111/geb.12280

Zhang, Y., Wallace, J. M., & Battisti, D. S. (1997). ENSO-like interdecadal variability: 1900-93. *Journal of Climate*, *10*(5), 1004–1020. https://doi.org/10.1175/1520-0442(1997)010<1004:ELIV>2.0.CO;2

Zhao, M., Mercer, J. L., Eglinton, G., Higginson, M. J., & Huang, C. Y. (2006). Comparative molecular biomarker assessment of phytoplankton paleoproductivity for the last 160 kyr off cap Blanc, NW Africa. *Organic Geochemistry*, *37*, 72–97. https://doi.org/10.1016/j.orggeochem.2005.08.022

Zimmerman, A. R., & Canuel, E. A. (2000). A geochemical record of eutrophication and anoxia in Chesapeake Bay sediments: Anthropogenic influence on organic matter composition. *Marine Chemistry*, *69*(1), 117–137. https://doi.org/10.1016/S0304-4203(99)00100-0